Available online at www.sciencedirect.com
SCIENCE DIRECT®
Bioorganic Chemistry 31 (2003) 398–411
BIOORGANIC CHEMISTRY
www.elsevier.com/locate/bioorg

Novel bisubstrate analog inhibitors of serotonin *N*-acetyltransferase: the importance of being neutral

Weiping Zheng and Philip A. Cole*

Department of Pharmacology and Molecular Sciences, Johns Hopkins University School of Medicine, 725 North Wolfe Street, Baltimore, MD 21205, USA

Received 25 April 2003

Abstract

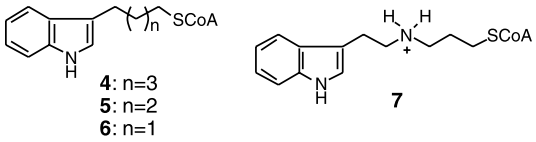

Linker modified novel bisubstrate analog inhibitors **4–7** for serotonin *N*-acetyltransferase (arylalkylamine *N*-acetyltransferase, AANAT) have been designed and synthesized. Examination of these inhibitors with AANAT in vitro suggested that: (i) linker hydrogen bonding makes only modest contributions to the affinity of bisubstrate analog inhibitors studied; (ii) greater than or equal to four methylene groups between the indole and the coenzyme A (CoASH) moieties are required for a bisubstrate analog inhibitor to achieve strong AANAT inhibition; (iii) the AANAT active site appears not to accommodate positively charged linkers as well as neutral ones; and (iv) substrate amine pK_a depression may constitute one strategy for AANAT substrate recognition and catalysis. The results reported here have enhanced our understanding of AANAT substrate recognition/catalysis, and are important for novel inhibitor design. Since AANAT belongs to the GCN5-related *N*-acetyltransferase (GNAT) superfamily, our experimental strategies should find applications for other acetyltransferases.
© 2003 Elsevier Science (USA). All rights reserved.

* Corresponding author. Fax: 1-410-614-7717.
E-mail address: pcole@jhmi.edu (P.A. Cole).

0045-2068/$ - see front matter © 2003 Elsevier Science (USA). All rights reserved.
doi:10.1016/S0045-2068(03)00081-6

Keywords: Serotonin *N*-acetyltransferase; Catalysis; Inhibitors; pK_a

1. Introduction

Serotonin *N*-acetyltransferase (arylalkylamine *N*-acetyltransferase, AANAT, EC 2.3.1.87) catalyzes the acetyl transfer from acetyl-coenzyme A (acetyl-CoA) to serotonin to form acetyl-serotonin (Fig. 1), which is the rate-limiting step in the biosynthesis of the circadian hormone melatonin (5-methoxy-*N*-acetyltryptamine) from serotonin [1]. Besides the natural substrate serotonin, AANAT also efficiently catalyzes acetyl transfer to other arylalkylamines such as tryptamine and phenethylamine.

The mechanism and inhibition of AANAT have drawn a lot of attention [2]. AANAT inhibitors are potential molecular probes for the biological roles played by the hormone melatonin, and these inhibitors may be potential therapeutics for sleep and mood disorders. Moreover, studies on AANAT may expand our understanding of the GCN5-related *N*-acetyltransferase (GNAT) superfamily which include some histone *N*-acetyltransferases and aminoglycoside *N*-acetyltransferases in addition to AANAT [3]. Studies on AANAT's catalytic mechanism have revealed it obeys an ordered Bi Bi sequential (ternary complex) mechanism with acetyl-CoA binding preceding arylalkylamine substrate [4]. These kinetic studies have led to the design and synthesis of AANAT bisubstrate analog inhibitors with two different linker types, i.e., amide- and ketone-linked compounds represented by **1**, **2**, and **3** (Fig. 2) [5]. Bisubstrate analog inhibitors have been used along with AANAT to solve the

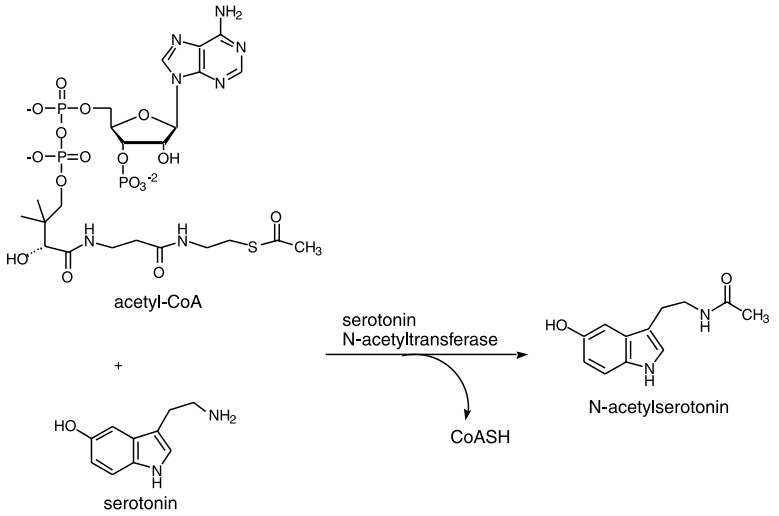

Fig. 1. AANAT-catalyzed acetyl transfer reaction.

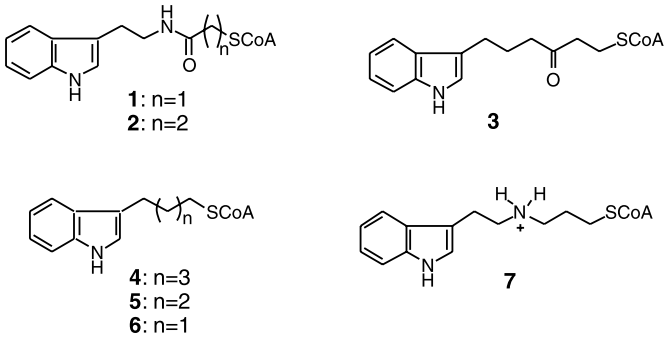

Fig. 2. The structures of AANAT bisubstrate analog inhibitors.

X-ray structure of the AANAT–bisubstrate analog complex which has shed further insight into molecular recognition and catalytic mechanism [6].

We were interested in further varying the linker structure in these bisubstrate analog inhibitors to potentially enhance inhibition and gain new mechanistic insights. Of note, the indole and coenzyme A (CoASH) moieties were kept intact in our design due to their mimicry of the substrates tryptamine and acetyl-CoA, respectively. These newly designed AANAT bisubstrate analog inhibitors (**4–7**, Fig. 2) allow us to explore the nature of hydrogen bonding and electrostatics in molecular recognition.

2. Materials and methods

2.1. General

All reagents for chemical synthesis were purchased from Aldrich. Reagents for enzyme inhibition assays were purchased from Sigma: CoASH, 5,5′-dithiobis(2-nitrobenzoic acid) (DTNB), *N*-(2-hydroxyethyl)piperazine-*N*′-(3-propanesulfonic acid) (EPPS) and assay-grade tryptamine hydrochloride; Pharmacia Biotech.: acetyl-CoA; Fisher Scientific: sodium phosphate, guanidinium hydrochloride, and EDTA. All commercially available reagents were used as purchased without further purification. ^{1}H NMR spectra were obtained with a Bruker AMX 300 spectrometer (300 MHz), and chemical shift values (δ) were expressed as parts per million (ppm) relative to tetramethylsilane (TMS). Electrospray ionization mass (ESI-MS) spectra were obtained with API 150EX (PE Biosystems). High resolution mass (HRMS) spectra were recorded on a MALDI DE-STR machine at the mass spectrometry facility of the University of California, Riverside. Silica gel (Merck, 63–200 mesh, 60 Å) was used for flash column chromatography. Analytical thin layer chromatography (TLC) was performed on Sigma-Aldrich silica gel 60 F 254 TLC plates (thickness: 200 μm). Preparative HPLC isolation of bisubstrate analog inhibitors was performed on a reverse-phase C-18 column (25×2.14 cm) (Microsorbtm-100, Rainin). Analytical HPLC used to monitor the progress of the CoASH

conjugation reactions with alkylhalides was performed on a reverse-phase C-18 column (25×0.46 cm) (Microsorb-MVTM-100, Rainin), eluted with a gradient of 50 mM aqueous potassium phosphate buffer (pH 4.5) (mobile phase A) and MeOH (mobile phase B) (0–3 min, 0% B; 3–15 min, linear increase to 65% B; 15–20 min, linear increase to 100% B; and 20–25 min, linear decrease to 0% B) (1.0 mL/min). All final bisubstrate analog inhibitors were >96% pure based on analytical HPLC profiles with two different solvent systems employing the same method. (i) 50 mM aqueous potassium phosphate buffer (pH 4.5) (mobile phase A) and MeOH (mobile phase B); (ii) water (0.05% TFA) (mobile phase A) and acetonitrile (0.05% TFA) (mobile phase B). The recombinant sheep glutathione *S*-transferase (GST)-serotonin *N*-acetyltransferase (GST-AANAT) (~90% pure) was expressed in *Escherichia coli* and purified by the glutathione–agarose affinity column, as described previously, and it has been shown that nearly identical acetyltransferase kinetic behavior was observed for GST-AANAT and GST-free AANAT [4]. Therefore, GST-AANAT was used for all the AANAT inhibition assays described in this report.

2.2. Synthesis of 1-bromo-5-(3-indolyl)pentane (**8**)

To a stirred cooled (ice-water bath) solution of 1-hydroxy-5-(3-indolyl)pentane (**12**) [7] (145 mg, 0.71 mmol) and carbon tetrabromide (390 mg, 2.1 mmol) in 3 mL of anhydrous Et_2O was added triphenyl-phosphine (309 mg, 1.19 mmol) in small portions. The reaction mixture was stirred at 0 °C for 15 min before the supernatant was collected and the oily residue was washed with Et_2O twice. The combined organic phases were concentrated in vacuo and the residue was subjected to silica gel flash column chromatography (EtOAc:hexane = 1:10; t.l.c. $R_f \sim 0.25$), affording 63 mg (33%) of **8** as a slightly yellow oil. ^{1}H NMR ($CDCl_3$) δ (ppm) 7.91 (bs, 1H), 7.60 (d, $J = 7.8$ Hz, 1H), 7.36 (d, $J = 8.4$ Hz, 1H), 7.19 (t, $J = 8.1$ Hz, 1H), 7.11 (t, $J = 7.4$ Hz, 1H), 6.99 (bs, 1H), 3.41 (t, $J = 6.9$ Hz, 2H), 2.78 (t, $J = 7.5$ Hz, 2H), 1.87–1.97 (m, 2H), 1.70–1.80 (m, 2H), 1.50–1.60 (m, 2H). ESI-MS: 266 ($[M + H]^+$).

2.3. Synthesis of 1-bromo-4-(3-indolyl)butane (**9**) [8]

(a) To a stirred cooled (ice-water bath) solution of 3-indolebutyric acid (408 mg, 2.0 mmol) in 3 mL of anhydrous THF was added dropwise $BH_3 \cdot$ THF (1.0 M in THF) (6.0 mL, 6.0 mmol) under N_2. The reaction mixture was stirred at room temperature for 3 h before water was added cautiously to destroy excess BH_3. THF was removed in vacuo and the product was extracted into EtOAc which was dried over anhydrous Na_2SO_4, filtered, and concentrated in vacuo. The resulting residue was subjected to silica gel flash column chromatography (EtOAc:hexane = 1:2), giving 230 mg (61%) of the intermediate 1-hydroxy-4-(3-indolyl)butane. ^{1}H NMR ($CDCl_3$) δ (ppm) 7.93 (bs, 1H), 7.61 (d, $J = 7.8$ Hz, 1H), 7.36 (d, $J = 8.1$ Hz, 1H), 7.19 (t, $J = 7.5$ Hz, 1H), 7.11 (t, $J = 7.4$ Hz, 1H), 6.99 (bs, 1H), 3.69 (t, $J = 6.6$ Hz, 2H), 2.80 (t, $J = 7.2$ Hz, 2H), 1.60–1.86 (m, 4H). (b) In the same manner as the synthesis of compound **8** from **12**, 48 mg (16%) of compound **9** was obtained as a brownish

solid from the above-obtained 1-hydroxy-4-(3-indolyl)butane (230 mg, 1.22 mmol) after silica gel flash column chromatography (EtOAc:hexane = 1:12; t.l.c. $R_f \sim 0.20$ in EtOAc:hexane 1:10). ^{1}H NMR ($CDCl_3$) δ (ppm) 7.91 (bs, 1H), 7.61 (d, $J = 7.5$ Hz, 1H), 7.36 (d, $J = 8.1$ Hz, 1H), 7.20 (t, $J = 7.5$ Hz, 1H), 7.13 (t, $J = 7.4$ Hz, 1H), 6.99 (bs, 1H), 3.45 (t, $J = 6.6$ Hz, 2H), 2.81 (t, $J = 7.5$ Hz, 2H), 1.81–2.06 (m, 4H).

2.4. Synthesis of 1-bromo-3-(3-indolyl)propane (**10**) [8]

In the same manner as the preparation of compound **9**, 62 mg (31%) of **10** was obtained from 3-indolepropionic acid (387 mg, 2.05 mmol) after two steps via the intermediate 1-hydroxy-3-(3-indolyl)propane. t.l.c. $R_f \sim 0.10$ in EtOAc:hexane 1:10; ^{1}H NMR ($CDCl_3$) δ (ppm) 7.95 (bs, 1H), 7.62 (d, $J = 7.8$ Hz, 1H), 7.37 (d, $J = 7.8$ Hz, 1H), 7.21 (t, $J = 7.5$ Hz, 1H), 7.13 (t, $J = 7.4$ Hz, 1H), 7.04 (bs, 1H), 3.45 (t, $J = 6.6$ Hz, 2H), 2.95 (t, $J = 7.2$ Hz, 2H), 2.21–2.31 (m, 2H).

2.5. Synthesis of N-chloropropyl-2-(3-indolyl)ethylamine (**13**)

To a stirred solution of tryptamine (352 mg, 2.2 mmol) in 4 mL of anhydrous tetrahydrofuran (THF) was added dropwise 1-bromo-3-chloropropane (99 μL, 1.0 mmol) under N_2 at room temperature. The mixture was stirred at 32–34 °C (2 h), 40–45 °C (6 h), and room temperature (overnight) before water was added to dissolve the precipitate formed. THF was removed in vacuo and EtOAc was added. The mixture was acidified with 6N aqueous HCl at 0 °C, and the water layer was washed with Et_2O to remove any unreacted 1-bromo-3-chloropropane before it was basified to c.a. pH 12 with a 6N aqueous NaOH solution at 0 °C. EtOAc was added and the resulting solution was washed with water, dried over anhydrous $MgSO_4$. EtOAc removal in vacuo afforded a brown oily residue which was subjected to preparative TLC (CH_2Cl_2:MeOH:NH_4OH = 100:10:2; $R_f \sim 0.6$), affording 77 mg (33%) of the isolated product **13** as a viscous colorless oil. ^{1}H NMR ($CDCl_3$) δ (ppm) 8.26 (bs, 1H), 7.63 (d, $J = 7.8$ Hz, 1H), 7.36 (d, $J = 8.1$ Hz, 1H), 7.20 (t, $J = 7.2$ Hz, 1H), 7.12 (t, $J = 7.4$ Hz, 1H), 7.03 (bs, 1H), 3.57 (t, $J = 6.6$ Hz, 2H), 2.98 (bs, 4H), 2.79 (t, $J = 6.9$ Hz, 2H), 1.88–1.97 (m, 2H). ESI-MS: 237 ($[M + H]^+$).

2.6. Synthesis of N-^{t}butyloxycarbonyl-N-chloropropyl-2-(3-indolyl)ethylamine (**14**)

To a stirred cooled (ice-water bath) suspension of **13** (53 mg, 0.224 mmol) in 1.5 mL of THF was added dropwise a solution of di-*tert*-butyl dicarbonate (49 mg, 0.225 mmol) in 0.5 mL of THF. The reaction mixture was heated at 50–62 °C for 1.5 h before THF was removed in vacuo. The resulting oily residue was subjected to preparative TLC (EtOAc:hexane = 1:3; $R_f \sim 0.5$), affording 24 mg (32%) of **14** as a viscous colorless oil. ^{1}H NMR ($CDCl_3$) δ (ppm) 8.04 (bs, 1H), 7.64 (d, $J = 7.5$ Hz, 1H), 7.36 (d, $J = 8.1$ Hz, 1H), 7.20 (t, $J = 6.9$ Hz, 1H), 7.12 (t, $J = 7.4$ Hz, 1H), 7.01 (bs, 1H), 3.51 (bs, 4H), 3.33 (bs, 2H), 3.00 (bs, 2H), 1.98 (bs, 2H), 1.35–1.52 (m, 9H). ESI-MS: 337 ($[M + H]^+$).

2.7. Typical procedure for the conjugation of CoASH with alkyl halides (**8–10**, **14**) to provide analogs **4**, **5**, **6**, and **15**

To a stirred solution of an alkyl halide in freshly degassed MeOH was added dropwise a solution of CoASH (0.5–1.0 equivalent) in a 1.0 M aqueous buffer solution of triethylammonium bicabonate (pH 8.1–8.5) at room temperature. The reaction mixture was stirred at room temperature or at 50–60 °C (for the conjugation between **7** and CoASH, where one equivalent of NaI was also present) for 15–24 h before MeOH was removed in vacuo. EtOAc was added to extract away any unreacted alkyl halide. The aqueous phase was lyophilized overnight, and the residue was subjected to preparative HPLC to isolate the desired products. The HPLC column was eluted with a gradient of 50 mM aqueous potassium phosphate buffer (pH 4.5) (mobile phase A) and MeOH (mobile phase B) (0–5 min, 0% B; 5–35 min, linear increase to 65% B; 35–50 min, linear increase to 100% B; and 50–55 min, linear decrease to 0% B) (10 mL/min), and was monitored at 260 nm. The isolated salt-containing product was desalted by the same preparative HPLC column eluted with double deionized (d.d.) water for 30 min, followed by MeOH to elute the product. The collected fractions were concentrated in vacuo and lyophilized to give the final products as white puffy solids which were characterized with ^{1}H NMR and HRMS, and used for the AANAT inhibition assays.

2.8. Analog **4**

By using the above-described typical conjugation procedure, analog **4** was prepared in 42% yield from compound **8**. HPLC t_R (19.2 min); ^{1}H NMR (CD_3OD) δ (ppm) 8.55 (s, 1H), 8.19 (s, 1H), 7.48 (d, $J = 7.8$ Hz, 1H), 7.30 (d, $J = 8.1$ Hz, 1H), 7.04 (t, $J = 6.9$ Hz, 1H), 6.98 (s, 1H), 6.95 (t, $J = 6.9$ Hz, 1H), 6.12 (d, $J = 6.0$ Hz, 1H), 4.86–4.98 (m, 2H), 4.49 (bs, 1H), 4.26 (t, $J = 5.1$ Hz, 2H), 4.07 (s, 1H), 4.00 (dd, $J = 9.6$, 5.4 Hz, 1H), 3.56 (dd, $J = 9.9$, 4.2 Hz, 1H), 3.46 (t, $J = 6.6$ Hz, 2H), 3.29 (t, $J = 6.6$ Hz, 2H), 2.72 (t, $J = 7.2$ Hz, 2H), 2.57 (t, $J = 7.2$ Hz, 2H), 2.51 (t, $J = 7.2$ Hz, 2H), 2.41 (t, $J = 6.9$ Hz, 2H), 1.65–1.75 (m, 2H), 1.55–1.65 (m, 2H), 1.40–1.52 (m, 2H), 1.06 (s, 3H), 0.82 (s, 3H). HRMS Calcd. for $C_{34}H_{51}KN_8O_{16}P_3S$ ($[M + K]^+$) 991.1994; Found: 991.2039.

2.9. Analog **5**

By using the above-described typical conjugation procedure, analog **5** was prepared in 20% yield from compound **9**. HPLC t_R (19.4 min); ^{1}H NMR (CD_3OD) δ (ppm) 8.55 (s, 1H), 8.19 (s, 1H), 7.49 (d, $J = 7.8$ Hz, 1H), 7.30 (d, $J = 8.1$ Hz, 1H), 7.04 (t, $J = 6.9$ Hz, 1H), 6.99 (s, 1H), 6.95 (t, $J = 6.9$ Hz, 1H), 6.12 (d, $J = 5.7$ Hz, 1H), 4.88–4.96 (m, 2H), 4.48 (bs, 1H), 4.26 (bs, 2H), 4.07 (s, 1H), 4.00 (dd, $J = 10.2$, 4.8 Hz, 1H), 3.56 (dd, $J = 9.6$, 3.9 Hz, 1H), 3.45 (t, $J = 6.9$ Hz, 2H), 3.28 (t, $J = 6.6$ Hz, 2H), 2.74 (t, $J = 6.9$ Hz, 2H), 2.55 (t, $J = 7.2$ Hz, 4H), 2.40 (t, $J = 6.9$ Hz, 2H), 1.72–1.84 (m, 2H), 1.55-1.69 (m, 2H), 1.06 (s, 3H), 0.81 (s, 3H). HRMS Calcd. for $C_{33}H_{49}KN_8O_{16}P_3S$ ($[M + K]^+$) 977.1837; Found: 977.1906.

2.10. Analog **6**

By using the above-described typical conjugation procedure, analog **6** was prepared in 25% yield from compound **10**. HPLC t_R (18.1 min); ^{1}H NMR (D_2O) δ (ppm) 8.55 (s, 1H), 8.20 (s, 1H), 7.65 (d, $J = 8.1$ Hz, 1H), 7.49 (d, $J = 8.1$ Hz, 1H), 7.24 (t, $J = 7.2$ Hz, 1H), 7.17 (s, 1H), 7.15 (t, $J = 7.2$ Hz, 1H), 6.17 (d, $J = 5.4$ Hz, 1H), 4.65 (bs, 1H), 4.31 (bs, 2H), 4.08 (s, 1H), 3.90 (dd, $J = 10.2$, 4.2 Hz, 1H), 3.62 (dd, $J = 9.9$, 4.5 Hz, 1H), 3.48 (t, $J = 6.3$ Hz, 2H), 3.34 (t, $J = 6.6$ Hz, 2H), 2.84 (t, $J = 7.2$ Hz, 2H), 2.67 (t, $J = 6.6$ Hz, 2H), 2.60 (t, $J = 7.2$ Hz, 2H), 2.44 (t, $J = 6.6$ Hz, 2H), 1.90–2.02 (m, 2H), 0.94 (s, 3H), 0.79 (s, 3H). HRMS Calcd. for $C_{32}H_{48}N_8O_{16}P_3S$ ($[M + H]^+$) 925.2122; Found: 925.2116.

2.11. Analog **15**

By using the above-described typical conjugation procedure, analog **15** was prepared in 8% yield from compound **14**. HPLC t_R (21.1 min); ^{1}H NMR (D_2O) δ (ppm) 8.53 (s, 1H), 8.20 (s, 1H), 7.61 (d, $J = 8.1$ Hz, 1H), 7.46 (d, $J = 7.8$ Hz, 1H), 7.21 (t, $J = 8.1$ Hz, 1H), 7.06–7.15 (m, 2H), 6.15 (d, $J = 5.4$ Hz, 1H), 4.62 (bs, 1H), 4.28 (bs, 2H), 4.05 (s, 1H), 3.87 (dd, $J = 10.2$, 4.2 Hz, 1H), 3.60 (dd, $J = 9.9$, 4.5 Hz, 1H), 3.47 (bs, 4H), 3.32 (bs, 2H), 3.02–3.28 (m, 2H), 2.95 (bs, 2H), 2.60 (bs, 2H), 2.40–2.50 (m, 4H), 1.52–1.78 (m, 2H), 1.42 (bs, 4H), 1.20 (bs, 5H), 0.92 (s, 3H), 0.78 (s, 3H). HRMS Calcd. for $C_{39}H_{59}N_9O_{18}P_3S$ ($[M - H]^-$) 1066.2912; Found: 1066.2992.

2.12. Analog **7**

To a stirred cooled (ice-water bath) solution of **15** (5 mg, 4.7 μmol) in 439 μL of d.d. water was added dropwise 430 μL of trifluoroacetic acid (TFA). The reaction mixture was stirred at room temperature for 105 min before it was basified to pH 8–9 using a 1.0 M aqueous triethylammonium bicarbonate buffer. The whole mixture was lyophilized overnight before it was subjected to preparative HPLC to isolate and desalt the product **7**. The HPLC methods used were the same as those for isolating/desalting analog **15**. 3.7 mg (81%) of analog **7** was obtained. HPLC t_R (15.0 min); ^{1}H NMR (D_2O) δ (ppm) 8.43 (s, 1H), 8.05 (s, 1H), 7.44 (d, $J = 7.8$ Hz, 1H), 7.32 (d, $J = 8.1$ Hz, 1H), 7.12 (s, 1H), 7.10 (t, $J = 8.1$ Hz, 1H), 7.00 (t, $J = 7.5$ Hz, 1H), 5.99 (d, $J = 3.0$ Hz, 1H), 4.54 (bs, 1H), 4.22 (bs, 2H), 3.96 (s, 1H), 3.79 (dd, $J = 10.2$, 4.5 Hz, 1H), 3.54 (dd, $J = 10.5$, 4.2 Hz, 1H), 3.41 (t, $J = 6.3$ Hz, 2H), 3.20–3.28 (m, 4H), 3.00–3.08 (m, 4H), 2.50 (t, $J = 6.6$ Hz, 4H), 2.39 (t, $J = 6.3$ Hz, 2H), 1.78–1.90 (m, 2H), 0.86 (s, 3H), 0.73 (s, 3H). HRMS Calcd. for $C_{34}H_{53}N_9O_{16}P_3S$ ($[M + H]^+$) 968.2544; Found: 968.2610.

2.13. Assay of AANAT inhibition by bisubstrate analog inhibitors **4–7**

AANAT activity was measured as described previously employing a spectrophotometric assay in which the enzymatic product CoASH concentrations were

Table 1
In vitro inhibition of AANAT acetyltransferase activity by bisubstrate analog inhibitors

Inhibitor	1	2	3	4	5	6	7
K_i (μM)[a]	0.048[b]	0.067[b]	0.032[c]	0.36	0.31	0.84	5.84

[a] Apparent inhibition constants (K_i) were derived from the Dixon plots, assuming all inhibitors are competitive versus acetyl-CoA, as demonstrated for analog **1** [5a]. The standard error for these measurements is estimated to be ±20%.
[b] See [9].
[c] See [5b].

determined indirectly by monitoring its reaction product with DTNB at 412 nm [4]. Assay reactions (pH 6.8 or 8.0) containing fixed concentrations of substrates acetyl-CoA (0.3 mM) and tryptamine (0.3 mM) (similar to their K_m values [4]), and at least five concentrations of a bisubstrate analog inhibitor (varied around K_i) were initiated with AANAT (14–56 nM) and the reactions were allowed to proceed for 2 min at 30 °C before being quenched with a 3.2 M aqueous guanidinium hydrochloride solution (pH 6.8). Rate measurements were made under initial conditions, i.e., limiting substrate turnover is $\leqslant$10%. All measurements were made in duplicate and data agreed within 20% in each duplicate run. A background (quenched before adding AANAT) was run for each inhibitor concentration. Inhibition kinetics were analyzed with Dixon plots that were shown to be linear in all cases. Apparent inhibition constants (K_i) (Table 1) were estimated from the Dixon plots, assuming all inhibitors are competitive versus acetyl-CoA and non-competitive versus tryptamine, as demonstrated previously for analog **1** [5a]. Although these K_i values are only approximate for inhibitors with slow-binding behavior that has been described for analog **1**, the prototype of this class of bisubstrate analog inhibitors reported in this work and previously [5b,9], good agreement between the K_i obtained from this analysis and the K_i* obtained from more extensive time-course measurements has been demonstrated previously for analog **1** [9].

3. Results and discussion

Analogs **4–6** were designed to investigate the dependence of the inhibitory potency on the distance between the indole and the CoASH moieties in AANAT bisubstrate analog inhibitors without the complications of hydrogen bonding groups in the linker. Comparative studies of compound **1**, **2**, **3**, and **4** allow an estimate of the contribution of amide and ketone groups in the linker with respect to overall binding affinity. ''Reduction'' of the amide linkage of **2** to a 2° amino group gave analog **7**. An intriguing feature of analog **7** is its chargeable linker, as compared to the neutral ones in all other current AANAT bisubstrate analog inhibitors. Studies on **7** permit an examination of the effects of linker positive charge on binding interactions with AANAT. Furthermore, the ionization state of the linker amino group of enzyme-bound **7** at a certain pH can potentially reflect that of the amino

group of tryptamine (or the natural substrate serotonin) in the AANAT active site.

Analogs **4–6** were prepared from the coupling at room temperature between Co-ASH and the corresponding 3-indolealkylbromides (**8–10**) in a mixture of 1.0 M triethylammonium carbonate buffer (pH 8.1–8.5) and freshly degassed MeOH under N_2 (Scheme 1). The reaction progress was monitored with analytical HPLC, and the conjugates were isolated by preparative HPLC. 3-Indolealkylbromides **8–10** were synthesized according to the procedures in Schemes 2 and 3. Intermediate **12** was prepared from indole according to the literature scheme and conditions as described [7]. 3-Indolepentylbromide (**8**) was obtained by treating **12** with CBr_4 and PPh_3 in anhydrous Et_2O. Alkylbromide **9** and **10** were prepared from the corresponding 3-indolealkanoic acid using the literature scheme [8] with several modifications employed.

Scheme 4 depicts the synthesis of analog **7**. Controlled alkylation of tryptamine with 1-bromo-3-chloropropane in anhydrous THF gave in 33% of yield intermediate

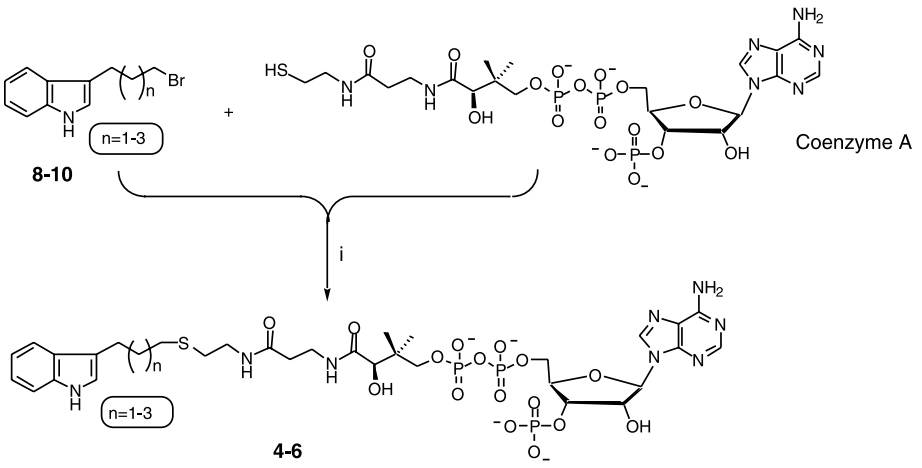

Scheme 1. (i) $Et_3NH^+ \cdot HCO_3^-$ (pH 8.1–8.5)/MeOH.

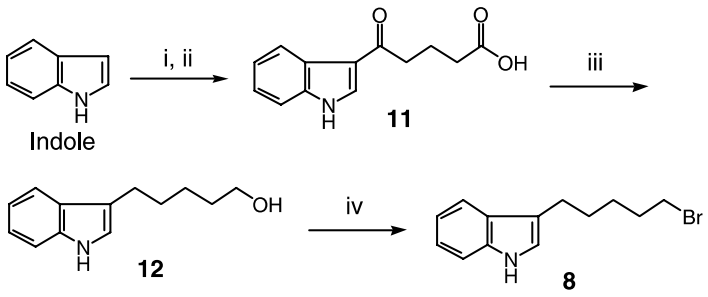

Scheme 2. (i) Mg, C_2H_5I, anisole; (ii) glutaric anhydride; (iii) $LiAlH_4$/THF; (iv) $CBr_4/PPh_3/Et_2O$.

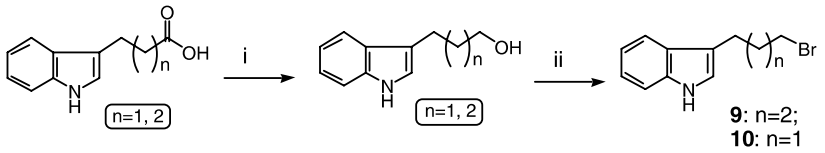

Scheme 3. (i) $BH_3 \cdot THF/THF$; (ii) $CBr_4/PPh_3/Et_2O$.

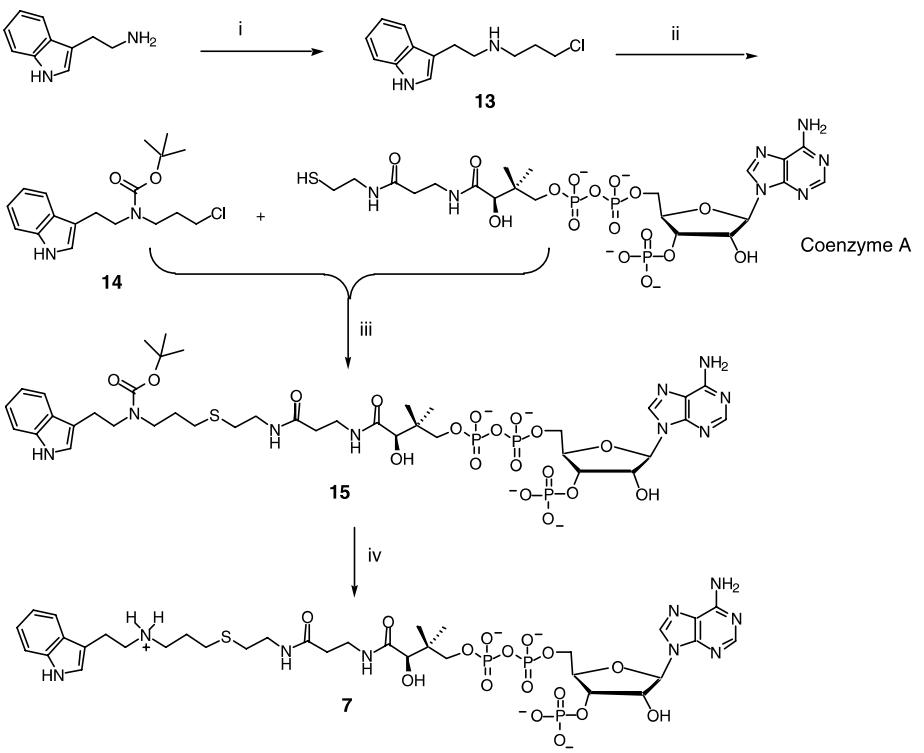

Scheme 4. (i) 1-bromo-3-chloropropane/THF; (ii) $(^tBoc)_2O$/THF; (iii) $Et_3NH^+ \cdot HCO_3^-$ (pH 8.4)/MeOH; (iv) TFA/H_2O (1:1).

13 whose secondary amino group was then protected as ^{t}Boc carbamide (**14**). The rather modest yield (32%) for this ^{t}Boc protection step may stem from competing intramolecular attack by the indole or amine. The coupling between CoASH and intermediate **14** was carried out in a mixture of 1.0 M triethylammonium carbonate buffer (pH 8.4) and freshly degassed MeOH at 50–55 °C under N_2. The reaction progress was monitored with analytical HPLC, and the product **15** was isolated by preparative HPLC. Treating precursor **15** with 50% aqueous trifluoroacetic acid (TFA) solution gave analog **7** that was isolated by preparative HPLC.

The identities of the final products (**4–7**) were confirmed by NMR and high resolution MS (HRMS) analyses.

Analogs **4–7** were evaluated as AANAT inhibitors on the purified sheep enzyme in vitro, as described previously [9]. Bioassay data were analyzed by Dixon plots, with results being recorded in Table 1.

The similar potency of inhibitors **1**, **2**, and **3** observed in our previous studies [5] suggested that the hydrogen bond between the amide nitrogen of **1** and the backbone carbonyl oxygen of Met159 on AANAT, observed on the structure of AANAT complexed with **1** [6b], is not energetically critical for inhibitor binding. However, it is possible that the amide carbonyl group contributes to the inhibitor binding affinity by hydrogen bonding to the backbone amide NH of L124 on AANAT, as observed in the co-crystal structure of AANAT and **1** [6b]. It is apparent from Table 1 that inhibitor **4** is 5- to 10-fold less potent as compared to inhibitors **1**, **2**, and **3**. This suggested that the hydrogen bond acceptor capability of the carbobyl group is likely to be worth approximately 1.4 kcal/mol in enhancing affinity.

The essentially identical inhibitory potency (K_i) for analogs **4** and **5** suggested that the linkers of these compounds can each confer the necessary optimal spacing and orientation of the indole and CoASH moieties for binding to AANAT. However, the increased spacing in compound **4** versus **5** may induce offsetting effects such as increased hydrophobic interactions with AANAT mediated by **4** but greater entropic loss due to its longer and more flexible linker.

The 2.5-fold decreased inhibitory potency of **6** as compared to **4** or **5** suggest that optimal orientation of the indole and CoASH moieties for enzyme binding is difficult to reach by shortening the linker length further. This observation further implies that, in contrast to arylethylamines [2a], arylmethylamines should serve as poor substrates of AANAT. It is conceivable that, in order for acetylation to occur, these poor substrates have to be pulled away from the optimal binding environment.

When we designed inhibitor **7**, we considered the plausible mechanistic model that arylalkylamine substrate binds to AANAT as the positively charged ammonium salt and is subsequently deprotonated by a general base during catalysis [2,10]. Under these circumstances, the bisubstrate analog inhibitor **7** might be expected to display higher binding affinity as compared to the neutral amide-linked inhibitor **1** or **2** (Fig. 2). However, **7** was observed to be a 122-fold weaker inhibitor than **1** and **2**. This observation suggested that the enzyme appears to have a preference for the binding of linker uncharged bisubstrate analogs rather than positively charged ones. Since "charge-neutral" hydrogen bonds tend to be more energetically favorable than "neutral–neutral" [11], these results suggest that the contribution of linker NH hydrogen bonding to bisubstrate analog affinity are not dominant. Indeed, as mentioned above, prior results with the ketone analog **3** indicated that the amide nitrogen in the linker was not critical for affinity [5b].

Further insight into the ionization state of the linker amine of **7** in the AANAT active site and the importance of hydrogen bonding is provided by comparing the behaviors of compounds **4** and **7**. Analog **4** lacks the NH-group from the linker in analog **7** but is otherwise a nice isostere. Analog **4** was shown to be a 16-fold stronger inhibitor than analog **7**. Since the affinity of **1, 2**, and **3** for AANAT are very similar, we reasoned that it is the presence or absence of the potential for positive charge on the linker of **7** versus **4** that results in the observed difference in binding affinity [12].

It is not unreasonable to expect that the interactions of indole and CoASH moieties with AANAT are conserved for inhibitors **1**, **2**, **3**, **4**, and **7**. Indeed, essentially identical AANAT complexes with **1**, **2**, or **7** were observed in X-ray crystallography studies (S. K. Burley and PAC, unpublished results). This structural conservation should also justify our assumption that all inhibitor **1**-related bisubstrate analog inhibitors were competitive versus substrate acetyl-CoA and non-competitive versus substrate tryptamine, as demonstrated for **1** [5a], and expected for AANAT which obeys an ordered Bi Bi kinetic mechanism. Thus, it is deduced that the positively charged form of **7** binds AANAT 16-fold more weakly than the neutral form of **7**. Based on Eq. (1) which should hold at low pH (6.8) when the linker amine is largely protonated in free solution:

$$[\text{amino-p}K\text{a (active site)}] - [\text{amino-p}K\text{a (free solution)}] = \log[(K_i\text{-}\mathbf{4})/(K_i\text{-}\mathbf{7})] \quad (1)$$

we estimate that the pK_a is ~1.2 lower for the linker amino group of inhibitor **7** in the AANAT active site versus in free solution.

Inhibitors **7** and **4** were further evaluated at a higher pH (8.0). A 60-fold decrease in potency was observed for inhibitor **4** at pH 8.0 versus pH 6.8, however, the corresponding decrease was 30-fold for inhibitor **7**. These results further support the concept that linker amine pK_a depression is associated with the binding of inhibitor **7** to the AANAT active site. The drastic decrease in affinity of **4** for AANAT likely results from AANAT ionizable groups that affect binding at the indole and/or the CoASH sites. Thus, changes in ionization from one or more groups of AANAT appear to weaken the interaction between AANAT and both bisubstrate analogs **4** and **7** as the pH is raised from 6.8 to 8.0. However, this weakening is modestly offset by the presumed increased proportion (by ~12%, assuming pK_a 8.8, see below) at pH 8.0 versus 6.8 of the neutral linker form of inhibitor **7** which is assumed to have 16-fold higher affinity for AANAT. Since tryptamine has a pK_a of 10 for its primary amino group in free solution [13], it is calculated that the AANAT active site likely depresses the substrate amine pK_a from 10 to ~8.8 (see Eq. (1)). These findings suggest that substrate amine pK_a depression and general base-mediated substrate ammonium ion deprotonation may work synergistically during AANAT substrate recognition and catalysis. AANAT may use general base(s) to directly or indirectly (via one or more water molecules) deprotonate the substrate ammonium ion [2b,6]. His120 and/or His122 may serve as the general base(s) [2b,6]. The maximum that a general base might be expected to contribute to rate enhancement at pH 7 is 60-fold. This is calculated based on the fact that about 1/60th of the tryptamine (assuming pK_a 8.8 in the active site) is already the neutral amine at pH 7. Such a 60-fold rate enhancement is in fair agreement with the effect (40-fold) observed with the double His to Gln mutant [2b].

In summary, linker modified novel AANAT bisubstrate analog inhibitors **4–7** have been designed and synthesized. Evaluation of these inhibitors with AANAT in vitro has suggested that: (i) linker hydrogen bonding makes only modest contributions to the affinity of bisubstrate analog inhibitors studied; (ii) greater than or

equal to four methylene groups between the indole and CoASH moieties are required for a bisubstrate analog inhibitor to achieve strong AANAT inhibition; (iii) the AANAT active site appears not to accommodate positively charged linkers as well as neutral ones; and (iv) substrate amine pK_a depression may constitute one strategy for AANAT substrate recognition and the catalysis. The results reported here have enhanced our understanding of AANAT substrate recognition and catalysis and will guide future inhibitor design. Since AANAT belongs to the GNAT superfamily, our experimental strategies and conclusions may extend to other important acetyltransferase enzymes.

Acknowledgments

Financial support from the Ellison Medical Foundation and National Institutes of Health are highly appreciated. The NMR studies were performed in the Biochemistry NMR Facility at Johns Hopkins University, which was established by a grant from the National Institutes of Health (GM 27512) and a Biomedical Shared Instrumentation Grant (1S10-RR06262-0).

References

[1] (a) D.C. Klein, J.L. Weller, Science 169 (1970) 1093–1095;
(b) S.L. Coon, P.H. Roseboom, R. Baler, J.L. Weller, M.A. Namboodiri, E.V. Koonin, D.C. Klein, Science 270 (1995) 1681–1683;
(c) J. Borjigin, M.M. Wang, S.H. Snyder, Nature 378 (1995) 783–785;
(d) D.C. Klein, P.H. Roseboom, S.L. Coon, Trends Endocrinol. Metab. 7 (1996) 106–112;
(e) D.C. Klein, S.L. Coon, P.H. Roseboom, J.L. Weller, M. Bernard, J.A. Gastel, M. Zatz, P.M. Iuvone, I.R. Rodriguez, V. Begay, J. Falcon, G.M. Cahill, V.M. Cassone, R. Baler, Recent Prog. Horm. Res. 52 (1997) 307–357.
[2] (a) W. Zheng, P.A. Cole, Curr. Med. Chem. 9 (2002) 1187–1199;
(b) K.A. Scheibner, J. De Angelis, S.K. Burley, P.A. Cole, J. Biol. Chem. 277 (2002) 18118–18126;
(c) N. Beaurain, C. Mesangeau, P. Chavatte, G. Ferry, V. Audinot, J.A. Boutin, P. Delagrange, C. Bennejean, S. Yous, J. Enzyme Inhib. Med. Chem. 17 (2002) 409–414.
[3] (a) D.E. Sterner, S.L. Berger, Microbiol. Mol. Biol. Rev. 64 (2000) 435–459;
(b) F. Javier Teran, M. Alvarez, J.E. Suarez, M.C. Mendoza, J. Antimicrob. Chemotherapy 28 (1991) 333–346.
[4] J. De Angelis, J. Gastel, D.C. Klein, P.A. Cole, J. Biol. Chem. 273 (1998) 3045–3050.
[5] (a) E.M. Khalil, P.A. Cole, J. Am. Chem. Soc. 120 (1998) 6195–6196;
(b) C.M. Kim, P.A. Cole, J. Med. Chem. 44 (2001) 2479–2485.
[6] (a) A.B. Hickman, D.C. Klein, F. Dyda, Mol. Cell 3 (1999) 23–32;
(b) A.B. Hickman, M.A. Namboodiri, D.C. Klein, F. Dyda, Cell 97 (1999) 361–369;
(c) E. Wolf, J. De Angelis, E.M. Khalil, P.A. Cole, S.K. Burley, J. Mol. Biol. 317 (2002) 215–224.
[7] A.H. Jackson, B. Naidoo, Tetrahedron 25 (1969) 4843–4852.
[8] E. Benghiat, P.A. Crooks, J. Med. Chem. 26 (1983) 1470–1477.
[9] E.M. Khalil, J. De Angelis, M. Ishii, P.A. Cole, Proc. Natl. Acad. Sci. USA 96 (1999) 12418–12423.
[10] E.M. Khalil, J. De Angelis, P.A. Cole, J. Biol. Chem. 273 (1998) 30321–30327.
[11] A.R. Fersht, J.P. Shi, J. Knill-Jones, D.M. Lowe, A.J. Wilkinson, D.M. Blow, P. Brick, P. Carter, M.M. Waye, G. Winter, Nature 314 (1985) 235–238.

[12] Even though the linker of analog **7** is slightly longer than that of **4**, it is reasonable to expect that this linker length variation per se does not contribute to the observed binding affinity difference between **7** and **4** based on our previous finding that elongation of the linker in **1** by one methylene group (giving analog **2**) has minimal impact on binding affinity [9]
[13] Merck and Co., Merck Index, nineth ed., Rahway, NJ (1976) 1095.